ZEPHYR

Towards a more efficient exploitation of on-shore and urban wind energy resources

Research and Innovation Action
Call: H2020-ITN-2019-1
Call topic: MSCA-ITN-2019 - Innovative Training Networks
Project start: 1 November 2019 Project duration: 48 months

D2.8: Rotor aerodynamics, acoustics and structural dynamics: final public report (T2.1-)

Executive summary
The ESRs focusing their research on rotor aerodynamics, acoustics and structural dynamics have collaborated to the development, improvement and cross-validation of a panel of methods for the prediction of the aerodynamic performance, noise emissions and structural behaviour of the WT type (HAWT, VAWT) their work has focused on. In addition, discussions relative to these turbine technologies held during previous workshops and meeting have been added to the content of this deliverable.

Partner in charge: NTU

Project co-funded by the European Commission within Horizon 2020 Dissemination Level		
PU	Public	PU
PP	Restricted to other programme participants (including the Commission Services)	–
RE	Restricted to a group specified by the Consortium (including the Commission Services)	–
CO	Confidential, only for members of the Consortium (including the Commission Services)	–

This project has received funding from the European Union's Horizon 2020 research and innovation programme under grant agreement No 860101

Deliverable Information

Document administrative information	
Project acronym:	**ZEPHYR**
Project number:	**860101**
Deliverable number:	**2.8**
Deliverable full title:	**Rotor aerodynamics, acoustics and structural dynamics: final public report**
Deliverable short title:	**Work Package 2 Final Public Report**
Document identifier:	**ZEPHYR-28-Work Package 2 Final Public Report-T21–Final version-v1.1**
Lead partner short name:	**NTU**
Report version:	**v1.1**
Report submission date:	**30/04/2023**
Dissemination level:	**PU**
Nature:	**[Report, Prototype, Other]**
Lead author(s):	**S. Shubham (NTU)**
Co-author(s):	**S. Sachar (IMP-PAN), A. Piccolo (TUD), A. Bresciani (CSTB), U. Boatto (SISW), O. Marino (UPM), L. Botero-Bolívar (UTW), K. Venkatraman (VKI)**
Status:	**Final version**

The ZEPHYR Consortium partner responsible for this deliverable has addressed all comments received. Changes to this document are detailed in the change log table below.

Change log

Date	Version number	Author/Editor	Summary of changes made
10/04/2023	v1.0	S. Shubham (NTU)	1st Draft report
20/04/2023	v1.1	S. Shubham (NTU)	2nd Draft report

Table of Contents

1 Introduction

Renewable energy sources have gained significant attention in recent years, and wind energy has been identified as one of the most promising sources of renewable energy. In particular, wind turbines have become increasingly popular due to their ability to generate electricity in a cost-effective and environmentally friendly manner. The design of wind turbines plays a crucial role in their efficiency and effectiveness in harnessing wind energy in a complex terrain or an urban environment. The two most common designs of wind turbines are horizontal axis wind turbines (HAWT) and vertical axis wind turbines (VAWT). HAWTs have rotor blades that rotate about a horizontal axis, while VAWTs have rotor blades that rotate about a vertical axis.

This report focuses on the latest developments in rotor aerodynamics, acoustics, and structural dynamics of HAWTs and VAWTs as part of the zEPHYR project. It highlights the latest developments in the research work carried out in the past 3 years, ultimately aimed at improving the design of such wind turbines. The report also explores the key challenges faced by the researchers and the possible solutions that can be implemented to overcome these challenges. The findings of this report are expected to contribute to the development of more efficient and effective wind turbines, which can play a significant role in meeting the growing demand for renewable energy.

One of the primary advantages of HAWTs is their higher efficiency in converting wind energy into electrical power. This is because HAWTs can capture wind energy from a larger area of the rotor, can operate at higher rotational speeds and can be placed in windier locations, such as coastal regions and offshore locations. However, the high rotational speeds can also result in noise and vibrations, which can be a significant issue in urban areas. In contrast, VAWTs have a lower efficiency due to the smaller rotor area that they can capture wind energy from, which limits their power output. However, VAWTs have a simpler design and can operate at lower wind speeds than HAWTs and have less noise and vibrations, making them more suitable for use in urban areas.

The contents of the document are the following: Section 2 presents latest updates for Horizontal Axis Wind Turbines (HAWTs) and Section 3 presents latest updates for Vertical Axis Wind Turbines (HAWTs). The report ends with conclusions for the report in Section 4 and acknowledgements in Section 5.

2 Horizontal Axis Wind Turbines (HAWTs)

2.1 Influence of blade deflections on wind turbine noise directivity

Fast turn-around methods are used in a framework of integrated aeroelastic and aeroacoustic simulations: the blade element momentum theory is coupled with a RANS-informed Amiet's model for the aeroacoustic modelling of trailing- and leading-edge noise. The workflow depicted in Figure 1 is applied to the NREL 5 MW wind turbine and the results of rigid and flexible blades are compared. Figure 2 shows the overall sound pressure level computed with flexible blades increases up to 13 dBA for listeners close to the rotor plane. This effect is attributed to the flapwise angular deflection of the wind turbine blade. Furthermore, the symmetry of the results with respect to the rotor plane is lost when the flapwise deflection is considered, indicating that the implementation of the blade deflections for the noise simulations should be considered for large wind turbines, which undergo significant blade deflections. For the NREL 5-MW wind turbine considered in this work, the trailing-edge noise is the dominant noise source. The leading-edge noise contribution becomes significant only at high wind speed and low frequency. Furthermore, its contribution to the total noise is relevant in the downwind and crosswind directions.

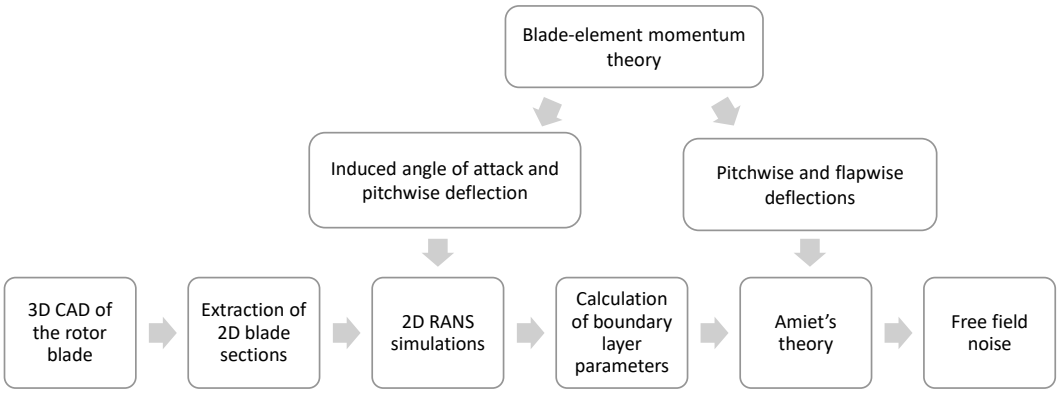

Figure 1: Diagram of the numerical workflow

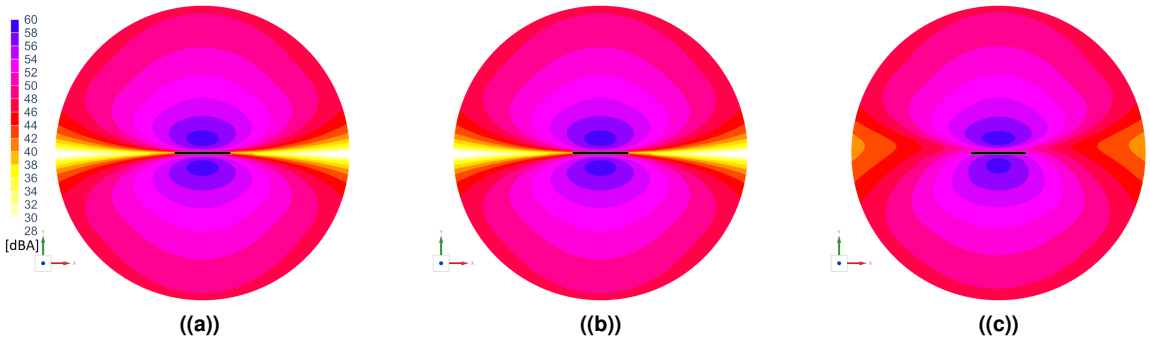

Figure 2: Footprint of the overall, A-weighted sound pressure level at rated conditions for the (a) rigid-blade simulation, (b) pitchwise-flexible blade simulation, and (c) fully-flexible blade simulation. The thick black line represents the rotor disk.

2.2 2D airfoils Noise Prediction Enhancement

2.2.1 LES simulations

Aerodynamics and aeroacoustic of wind turbines are modeled based on 2D airfoil data. To improve this model, a better understanding of airfoil physics, including turbulence is needed. In the following section, numerical and experimental assessment of this problem are presented, including guidelines for high fidelity simulations and interaction with inflow turbulence.

For the assessment of the numerical simulation, we perform Large Eddy Simulation on a 3D NACA0012 airfoil using a high order discontiuous Galerkin spectral element solver. This airfoil is simulated at moderate Reynolds numbers, $Re = 1.0 \cdot 10^5$ and a low angle of attack, of $AoA = 4.0°$. The aim is to compare the results of classic explicit Sub Grid Scale, with the ones get by using implicit LES, where no explicit SGS is used, but we use stabilising split-form energy-stable formulations.

The WALE model predicted the transition to turbulence before mid-cord position, with a very small recirculation zone at in the upstream (at $x/C \approx [0.1, 0.3]$). In contrast, the VREMAN model produces clearer laminar recirculation bubbles that are mostly 2D and evolve into corrugated 3D structures which become later on turbulent structures at the vicinity of the trailing edge. As for the iLES cases, both show the correct behaviour, with a larger 2D laminar separation bubble until transition occurs (at $x/C \approx 0.6$). Overall we observe that all these LES techniques predict a laminar region, transition to turbulence and turbulence separation.

2.2.2 Study of the increase of trailing-edge noise due to inflow turbulence for enhancing trailing-edge noise prediction methods

The effect of inflow turbulence has mostly been focused on the so-called turbulence interaction noise mechanism. However, recent results show that the trailing-edge noise is also increased because of the free-stream turbulence penetration in the airfoil boundary layer. This research measures the increase of trailing-edge noise due to inflow turbulence for NACA 63018 and NACA 0008 airfoils. Noise measurements were conducted for velocities ranging from 15 to 40 m/s, with and without inflow turbulence. A rod installed upstream of the airfoils generated an inflow turbulence of $\approx$ 12%. The wall-pressure fluctuations were measured close to the trailing edge to analyze the near-field phenomenon. The inflow turbulence increases the wall-pressure spectrum level in the entire frequency range and the spanwise correlation length in the low-frequency range. The trailing-edge noise increases due to the inflow turbulence in the entire frequency range at least 2 dB up to more than 15 dB for all the cases. The contribution of leading- and trailing-edge noise to the total noise varies with the airfoil geometry, with the trailing-edge noise dominating in a larger frequency range for the thickest airfoil

2.2.3 Turbulence distortion investigation for leading-edge noise prediction methods enhancement

A novel approach to account for the effects of turbulence distortion in the prediction of leading-edge noise has been proposed. The analytical model developed by Amiet has been modified by considering in input a turbulence spectrum sampled in the flow-field region where the distortion occurs, to consider the alterations experienced by the velocity components near the airfoil leading edge and, consequently, their impact on the far-field noise.

A rod-airfoil configuration has been selected to carry out the analysis of the vortex dynamics and generalize the acoustic investigation considering both broadband and tonal sound components. The trend of the root-mean-square values of the velocity fluctuations along the stagnation streamline in the vicinity of the airfoil leading edge are consistent with the results of the Rapid Distortion Theory (RDT): the vertical-velocity component increases substantially at the expense of the horizontal one, which must decrease because of the no-penetration condition. The analysis of the band-pass filtered velocity fluctuations has shown that these distortion mechanisms start occurring at a distance from the stagnation point related to the size of the turbulent structures. This result suggests that turbulence distortion is not occurring within a distance from the body related to a geometrical characteristic but depends on the inherent dimensions of the scales involved in the interaction.

The surface pressure in the midspan plane have also been considered to investigate the effects of turbulence distortion on the noise generation. From the analysis of the root-mean-square values, it arose that the highest surface-pressure fluctuations are obtained downstream of the stagnation point, at the position where the pressure gradient along the airfoil is peaking. This observation allows linking a quantity related to the noise generation as the pressure fluctuations with the mean flow behavior along the surface of the airfoil. In particular, it indicates that the noise-generation efficiency is related to the intensity of the pressure gradient and, hence, the flow acceleration around the leading edge.

The results of this physical study have been therefore used to modify Amiet's model by sampling the turbulence spectrum at the position where the pressure fluctuations are the largest: this analytical method has shown good agreement with the numerical results obtained with the FW-H analogy, in terms of both sound pressure levels and directivity patterns 3.

This study represents a first step towards a more thorough understanding of the relation between turbulence distortion and leading-edge noise generation with the purpose of enhancing the noise prediction by means of low-fidelity methods. Yet further investigations are necessary to investigate the behavior of the different turbulent structures in the interaction with the airfoil and to define and corroborate the impact of this physical mechanism on the surface pressure distribution.

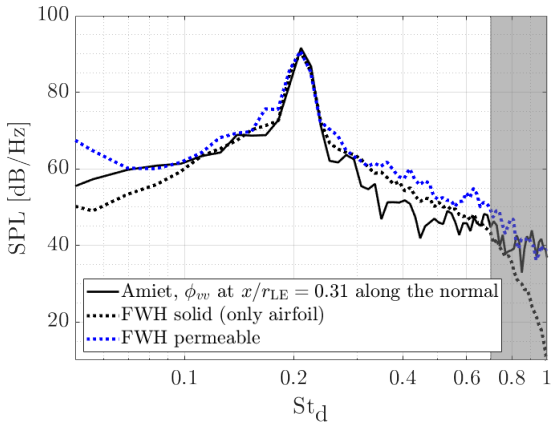

Figure 3: Sound spectrum in the far-field calculated for an observer placed at $R = 9.25\,c$ and $\theta = 90°$, with the angular position computed with respect to the downstream direction. The results of Amiet's implementation considering "distorted" spectrum in input are compared to the calculation provided by the solid formulation of the FW-H analogy. The reference pressure used to calculate the SPL is 2×10^{-5} Pa.

3 Vertical Axis Wind Turbines (VAWTs)

3.1 Effect of number of blades

The first study investigates the aerodynamics and aeroacoustics of small-scale Darrieus VAWTs operating at chord-based Reynolds numbers below 5×10^5. Four different VAWT configurations with varying numbers of blades (1, 2, 3, and 4) are considered, and a wide range of tip speed ratios (TSRs) is examined while maintaining a constant freestream velocity of 9 m/s. These values are chosen to resemble a reference simulation campaign (Balduzzi et al., 2018) for the purpose of validating the numerical results. The performance parameters of the VAWT, including thrust, torque, power, and overall sound pressure level (OSPL), are investigated. Fluid dynamic simulations are conducted using both mid-fidelity and high-fidelity computational fluid dynamics (CFD) methods. The mid-fidelity simulations are carried out using the open source software QBlade 2.0, which employs the unsteady Lifting Line Free Vortex Wake (LLFVW) method. The high-fidelity simulations are performed using the commercial software 3DS Simulia PowerFLOW 6-2020, which uses the Lattice Boltzmann/Very Large Eddy Simulation (LB-VLES) method for CFD calculations and the Ffowcs-Williams and Hawkings (FW-H) acoustic analogy to calculate the far-field noise.

The results indicate that increasing the number of blades enhances the power generated at lower TSRs, but this trend is reversed at higher TSRs. At low TSR, increasing solidity negligibly increases blade-wake/blade-vortex interaction, which in turn increases the total blade tangential loading and power produced. However, at higher TSR, increasing solidity decreases the tangential loading on each blade and the overall rotor power. Consequently, higher solidity leads to a sharper gradient in C_P values than lower solidity cases, over the whole range of TSR. Additionally, the optimal TSR decreases as the number of blades increases, as shown by C_P values.

To better understand the blade-wake and blade-vortex interactions and their effect on the overall rotor performance, visualizing the 3D VAWT flowfield is crucial. Figure 5 provides insight into instantaneous vortices in the downstream part of the VAWT flowfield using iso-surfaces of the λ_2 criterion. The visualization is done for TSR = 3.3. As the number of blades increases, the large vortex structures, consisting of the coherent shed and trailing (tip) vortices, and smaller incoherent vortex structures increase proportionately in the flowfield. The shed vortices originate at $0°$ and $180°$ azimuth and are due to the change in the direction of the airflow around the blade as it moves from downwind to upwind part of rotation and vice versa. The tip vortices convect downstream and create a spiral flow pattern, also known as "vortex ring", that wraps around the axis of the turbine. The density of these vortices in the vortex ring increases

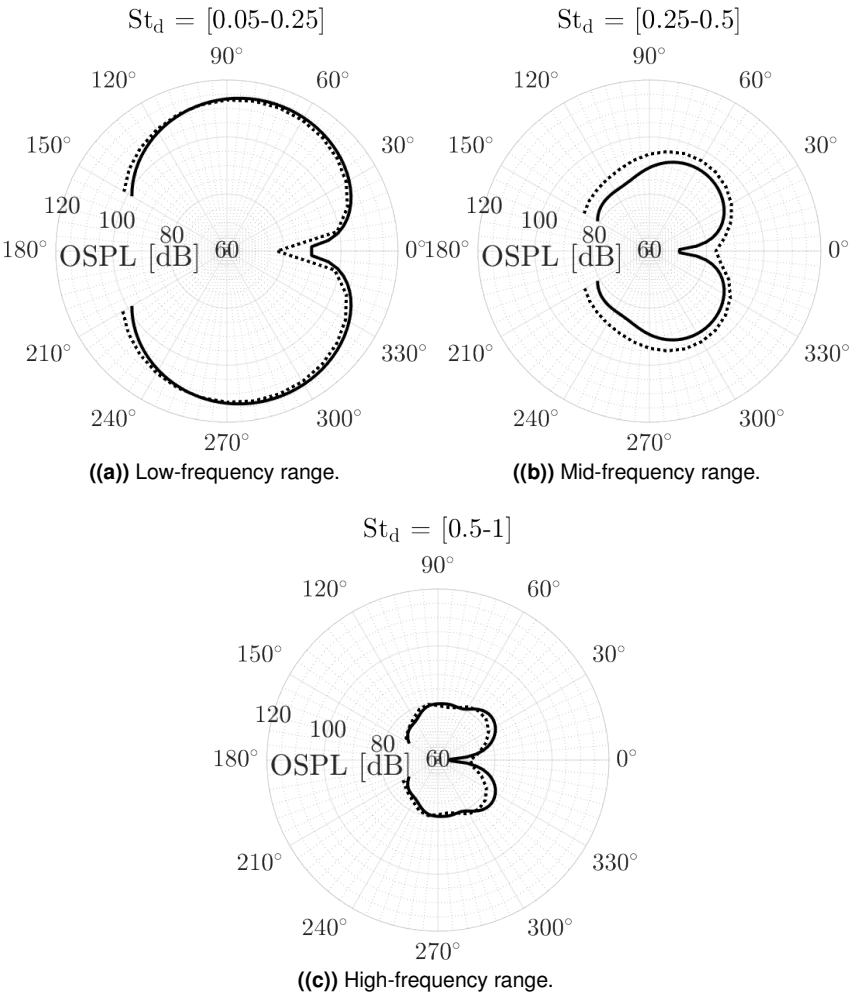

((a)) Low-frequency range.

((b)) Mid-frequency range.

((c)) High-frequency range.

Figure 4: Far-field noise directivity patterns. Comparison of the Amiet Model with the "distorted" spectrum in input and the FW-H solid results. For the legend, see Fig. 3.

as the number of blades increases.

As the large vortex structures convect downstream, they experience wake expansion and gradually break down into smaller-scale structures due to flow instabilities and spatial modulation, which eventually dissipate and are mixed into the surrounding fluid (Avallone, Ragni, & Casalino, 2020; Lignarolo, Ragni, Scarano, Ferreira, & Van Bussel, 2015). As the number of blades increases, the increase in blade vortex interaction leads to a disturbance in the ideal pressure and loading distribution along the chordwise and spanwise directions, resulting in the lower aerodynamic performance of the downstream blades as compared to the upstream blades which experience clean freestream flow.

Both the mid-fidelity LLFVW and high-fidelity LBM methods capture these physical trends very well. However, the LLFVW method under-predicts peak C_T and C_Q values in the upwind and downwind parts of the rotation as compared to LBM, except for the 2-bladed rotor. This discrepancy may be attributed to the LLFVW method's limited capability to capture the complex 3D effects in a VAWT flow and force field as strongly as LBM, particularly when the number of blades increases. The study suggests empirical modifications in the airfoil lift and drag polar values for the LLFVW method. The study also compared the aeroacoustic characteristics of all four VAWT configurations. It found that low-frequency BPF noise was higher in VAWTs with fewer blades due to the higher rotor loading or thrust values obtained, while high-frequency noise was higher in VAWTs with more blades due to a higher intensity of blade-wake/blade-

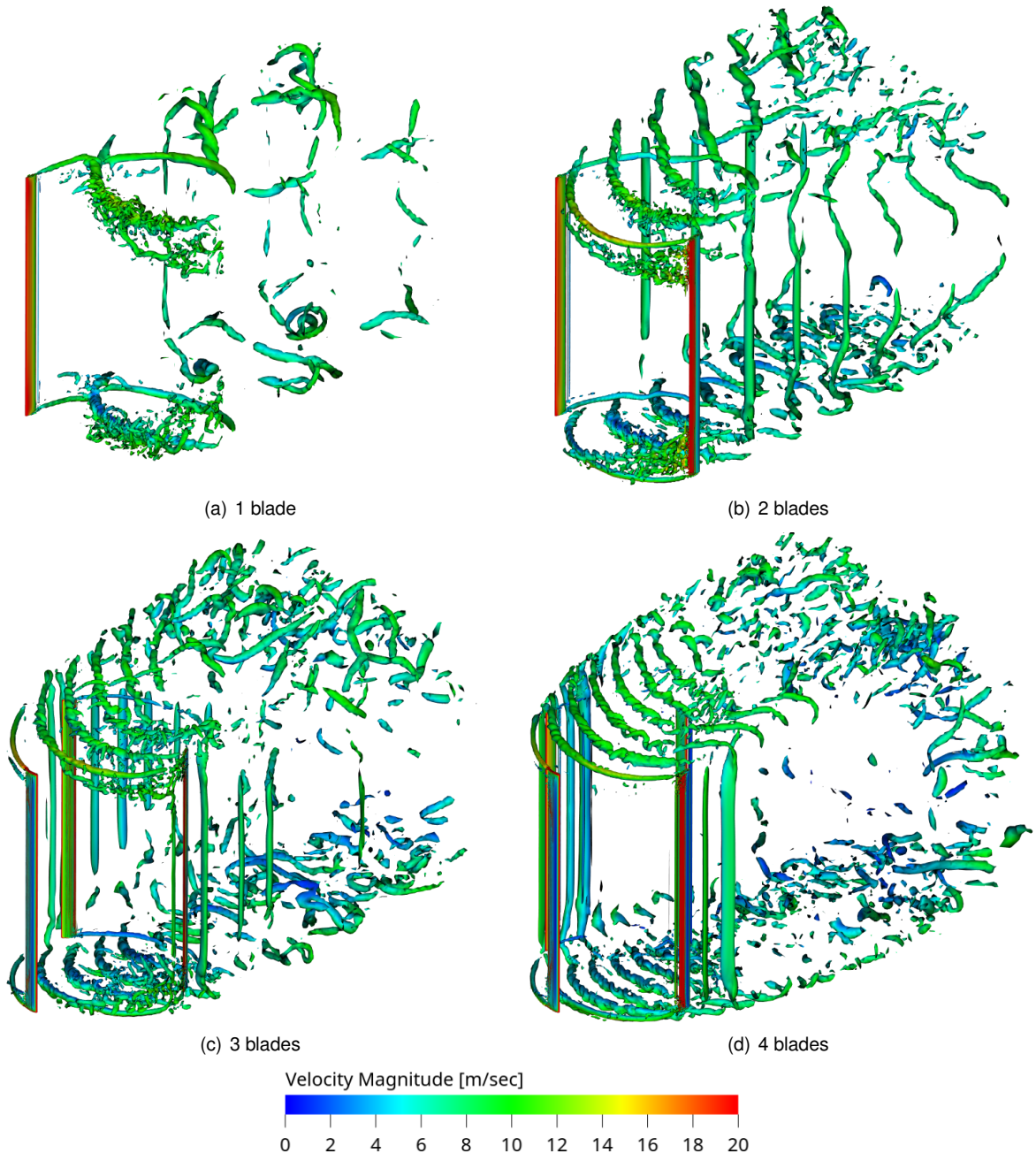

Figure 5: Instantaneous 3D flowfield using iso-surfaces of the λ_2 criterion for vortices visualization, using high-fidelity LBM, at TSR = 3.3; adapted from (Shubham, Ianakiev, et al., 2023)

vortex interaction between the downstream blades and previously shed blade vortices. A similar study is conducted to compare the results using low-fidelity streamtube model and mid-fidelity lifting line vortex model (Shubham, Naik, Sachar, & Ianakiev, 2023).

3.2 Grid independence study using Richardson extrapolation and the effect of tip speed ratio

The second study investigates the aerodynamics and aeroacoustics of small scale Darrieus VAWTs at chord-based Reynolds numbers below 1.5×10^5. A grid convergence study is conducted for thrust, cross-streamwise force and torque coefficient, and overall sound pressure level (OSPL) using four levels of grid refinement. The Richardson Extrapolation method is used to estimate the continuum value of each parameter using the three finest grids and to calculate the grid convergence level. Four operational points for the Darrieus VAWT are investigated, at tip speed ratios (TSRs) of 0.37, 1.12, 2.23, and 2.79, with a constant freestream velocity of 5.07 m/s, to resemble an experimental campaign to validate the numerical results. Commercial software 3DS Simulia PowerFLOW 6-2020 is used to perform high-fidelity CFD simulations, and the Ffowcs-Williams and Hawkings (FW-H) acoustic analogy to calculate the far-field noise. The results indicate that thrust, cross-streamwise force, and OSPL have better grid convergence than torque. Furthermore, grid convergence is better at TSR = 2.23 than at other TSRs. The study shows that blades in the downwind half of rotation produce less thrust and torque than in the upwind half, due to the effect of VAWT wake on the former. This is shown in Figure 6. The difference in values between the two halves increases with increasing TSR, in general, due to the wake getting stronger at higher TSR, with the ratio of contribution between upwind and downwind halves going as high as 17.6 in the case of thrust for TSR = 2.79. In terms of noise, higher TSR produces more noise than the lower TSR configuration due to an increase in unsteady blade loading with increasing TSR.

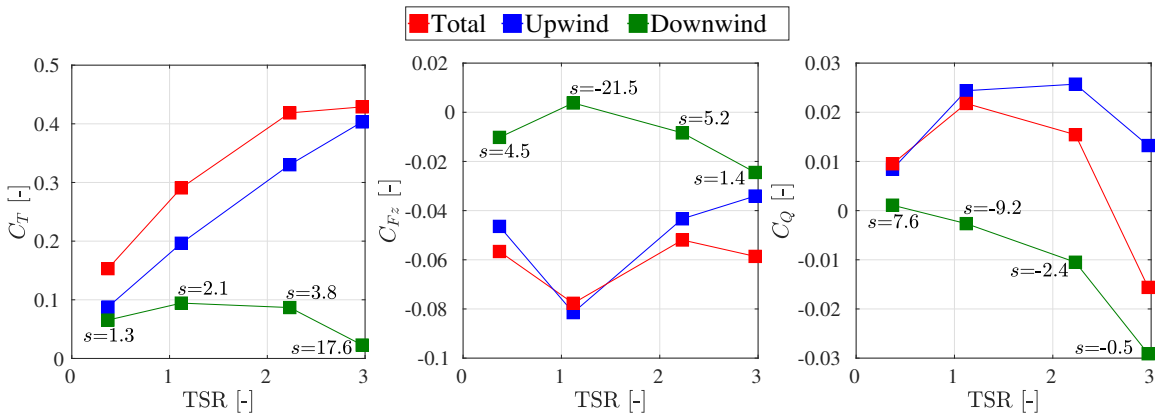

(a) Thrust coefficient C_T (b) Cross-streamwise force coefficient C_{Fz} (c) Torque coefficient C_Q

Figure 6: Comparison of integral values of a single blade for the full rotation with the upwind and downwind halves separately; s denotes ratio of contribution from upwind and downwind halves; adapted from (Shubham et al., 2022)

With regard to OSPL directivity on a circular array of points, noise is highest at the most upstream azimuth location corresponding to the location where blade loading is highest in a single rotation. This is shown in Figure 7.

3.3 Correlation Between the Generated Noise and Effectiveness for a Vertical Axis Savonius Type Rotor

Another investigation (Sachar et al., 2023) involves a comparison between a single segment rotor and a five segment rotor to determine the optimal rotor with minimum noise and maximum efficiency, in case of Savonius VAWT. The findings indicate that the five segment rotor generates lower overall noise than the single segment rotor. The noise level decreases with an increase in load and is maximum when the rotor is rotating freely. Under the given test conditions, the single segment rotor exhibits superior efficiency

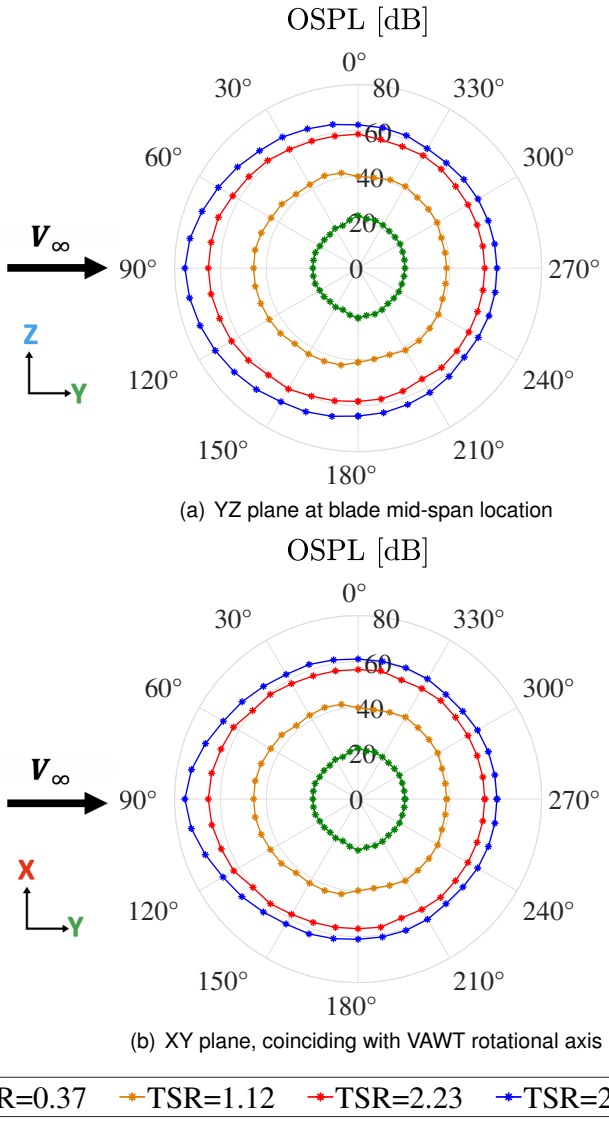

(a) YZ plane at blade mid-span location

(b) XY plane, coinciding with VAWT rotational axis

Figure 7: Directivity plot of overall sound pressure level (OSPL) comparing 4 different TSRs, along a circular array of 36 points situated at a distance of 7D from the origin of VAWT ([0,0,0]); adapted from (Shubham et al., 2022)

at a wind velocity of 8.5 m/sec, achieving a maximum performance efficiency of 32% in contrast to the 26.5% efficiency of the five-segment rotor.

However, the 10-fold increase in sound intensity level in the case of the single segment rotor is not desirable, considering the absolute decrease in maximum efficiency is approximately 6%. This is particularly true in urban environments where the safety and health of residents are of utmost importance. Consequently, the usage of a five segment rotor has reduced noise levels by 10 dB, albeit at the expense of efficiency loss.

Moreover, the investigation can be extended by mounting the rotor in a wind tunnel and measuring the noise solely from the rotor, eliminating any noise from the fan. Furthermore, the study can be expanded to consider different wind velocities. The selection of the rotor will also depend on the local regulations and the maximum permissible dB levels stipulated by the relevant authorities.

3.3.1 Influence of tip speed ratio on aeroacoustics of 3-bladed H-Darrieus VAWTs

This section is an extract taken from the work presented in (Venkatraman, Moreau, Christophe, & Schram, 2022). Noise generated by a 3 bladed complete scaled model H-Darrieus vertical axis wind turbine with end plates and supporting structures has been investigated using the LBM-VLES approach implemented in the commercial flow solver PowerFLOW.

Figure 8: Model VAWT rotor studied by (Weber et al., 2015).

The effect of increasing the TSR, which is the key parameter to define different flow regimes for VAWTs, is analyzed with the objective of obtaining the noise curve. Simulation data is shown for three different flow regimes: the deep stall regime at a low TSR of 0.4, the operational (maximum efficiency) regime at a TSR of 1.7 and the parasitic drag regime at a high TSR of 3. The wall pressure data on the blades is recorded and provided as an input to the FW-H analogy implemented in the in-house code SherFWH to compute the noise spectra. The variation of the OASPL is computed at an observer position located 1 m corresponding to an azimuthal position 0°. The OASPL values increases with increasing TSR.

As presented previously, negligible power is produced in the deep stall regime. The blades encounter high angles of attack and experience dynamic stall, more specifically in the upwind phase of rotation. Significant flow separation and dynamic stall structures are seen in this regime indicating the presence of important noise generation mechanisms such as dynamic stall noise and blade wake interaction noise. At low frequencies, the spectra is dominated by the tonal noise at the Blade passing frequency (BPF), while at mid and high frequencies the broadband components dominate. An excellent agreement is obtained between the present results and available experimental data for both the tonal and broadband components.

With increasing TSR, the power coefficient C_p reaches a peak corresponding to the operational regime. In this regime, the key flow features are the tip vortices and their interaction with the supporting structures. The flow features are comparable to a rotating spinning cylinder. A good agreement is seen between the present results and the available experimental data in this regime for the noise spectrum computed at the same observer position. The broadband noise levels at the mid and high frequencies increase when compared to the deep stall regime.

Further increasing the TSR leads to a decrease in the power coefficient leading to the parasitic drag regime. Strong blade wake interaction is seen in the parasitic drag regime at a high TSR, with the tip vortices interacting with the oncoming blades and supporting structures two or more times. Similar to the operational regime, the flow features exhibit similarity to a rotating spinning cylinder. There is an

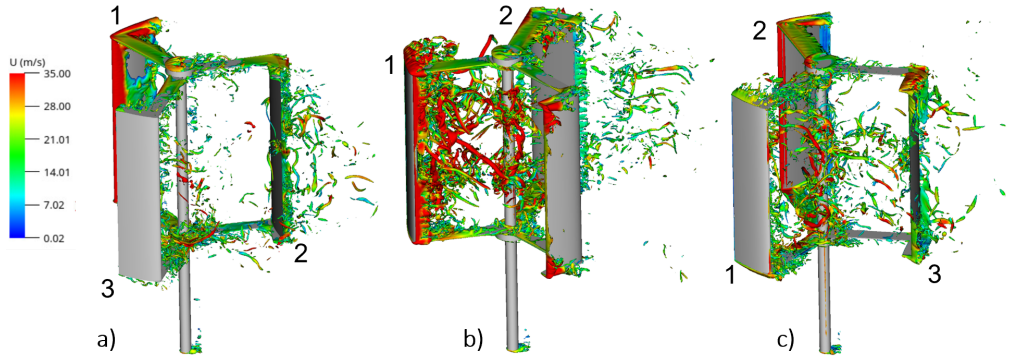

Figure 9: Iso-contours of Q-criterion for TSR = 0.4 at different azimuthal positions a) 45° b) 90° c) 135° corresponding to blade 1 for a iso-value of 13000.

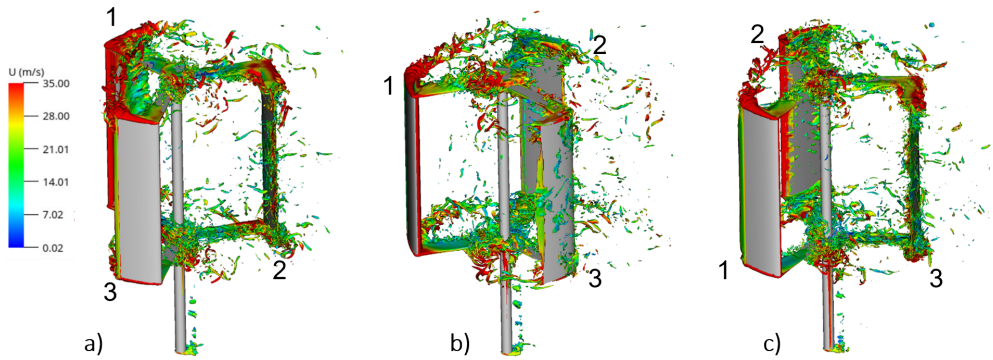

Figure 10: Iso-contours of Q-criterion for TSR = 1.7 at different azimuthal positions a) 45° b) 90° c) 135° corresponding to blade 1 for a iso-value of 13000.

increase in both the tonal and broadband noise levels compared to the other regimes. Additionally, for the selected observer position, the second BPF tone is found to be the most dominant. The increase in broadband noise with tip speed ratio is as expected, due to stronger and more frequent blade wake interactions.

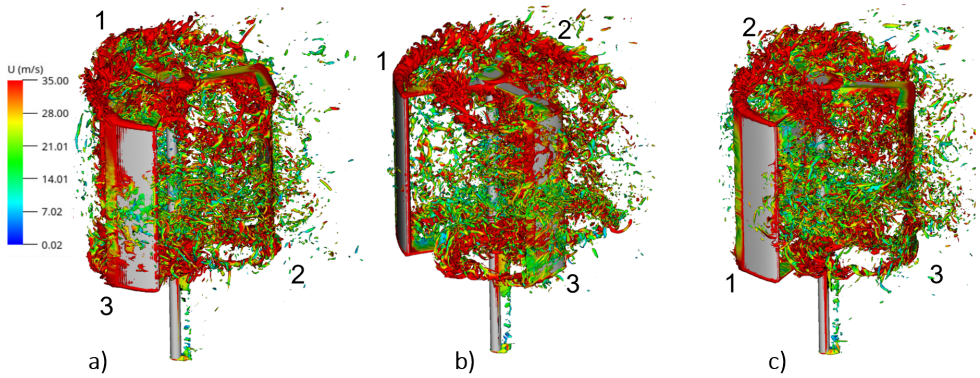

Figure 11: Iso-contours of Q-criterion for TSR = 3 at different azimuthal positions a) 45° b) 90° c) 135° corresponding to blade 1 for a iso-value of 13000.

4 Conclusions

This report has explored the latest developments in rotor aerodynamics, acoustics, and structural dynamics of horizontal axis wind turbines (HAWTs) and vertical axis wind turbines (VAWTs) as part of the zEPHYR project. It has highlighted the primary advantages and disadvantages of HAWTs and VAWTs and how they are suitable for specific applications. For instance, HAWTs have a higher efficiency in converting wind energy into electrical power but are associated with noise and vibration issues, making them more suitable for use in coastal regions and offshore locations. On the other hand, VAWTs have a simpler design and operate at lower wind speeds than HAWTs, making them more suitable for use in urban areas.

The report has also explored specific areas of research. The first is the influence of blade deflections on wind turbine noise directivity, where the report found that the implementation of blade deflections for noise simulations is critical for large wind turbines that undergo significant blade deflections. The second area of research is the enhancement of 2D airfoil noise prediction, where better understanding of airfoil physics, including turbulence, is essential to improve aerodynamics and aeroacoustics models of wind turbines. The third area of research is on the VAWTs, investigating grid convergence behaviour using Richardson extrapolation method, and the effect of tip speed ratios and number of blades on aerodynamic and aeroacoustic performance.

Overall, the findings of this report are expected to contribute to the development of more efficient and effective wind turbines, which can play a significant role in meeting the growing demand for renewable energy.

5 Acknowledgments

This project has received funding from the European Union's Horizon 2020 research and innovation programme under grant agreement No EC grant 860101. We are grateful to that and the members who are not listed as co-authors for their helpful discussions and comments.

References

Avallone, F., Ragni, D., & Casalino, D. (2020). On the effect of the tip-clearance ratio on the aeroacoustics of a diffuser-augmented wind turbine. *Renewable Energy*, *152*, 1317–1327.

Balduzzi, F., Marten, D., Bianchini, A., Drofelnik, J., Ferrari, L., Campobasso, M. S., ... Paschereit, C. O. (2018). Three-dimensional aerodynamic analysis of a darrieus wind turbine blade using computational fluid dynamics and lifting line theory. *Journal of Engineering for Gas Turbines and Power*, *140*(2).

Lignarolo, L., Ragni, D., Scarano, F., Ferreira, C. S., & Van Bussel, G. (2015). Tip-vortex instability and turbulent mixing in wind-turbine wakes. *Journal of Fluid Mechanics*, *781*, 467–493.

Sachar, S., Doerffer, P., Flaszynski, P., Kotus, J., Doerffer, K., & Grzelak, J. (2023). Correlation between the generated noise and effectiveness for a vertical axis savonius type rotor. In *Aiaa scitech 2023 forum* (p. 0611).

Shubham, S., Ianakiev, A., Avallone, F., & Wright, N. (2023). Effect of number of blades on aerodynamic and aeroacoustic characteristics of low reynolds number vertical axis wind turbines. In *2023 aiaa aviation forum.*

Shubham, S., Naik, K., Sachar, S., & Ianakiev, A. (2023). Performance analysis of low reynolds number vertical axis wind turbines using streamtube and vortex methods and wind conditions in the city of nottingham. *Accepted in Energy*.

Shubham, S., Wright, N., & Ianakiev, A. (2022). Application of richardson extrapolation method to aerodynamic and aeroacoustic characteristics of low reynolds number vertical axis wind turbines. In *28th aiaa/ceas aeroacoustics 2022 conference* (p. 3022).

Venkatraman, K., Moreau, S., Christophe, J., & Schram, C. (2022). Numerical investigation of the noise radiated by an H-Darrieus vertical axis wind turbine at different tip speed ratios. In *28th aiaa/ceas aeroacoustics conference, southampton.*

Weber, J., Becker, S., Scheit, C., & Grabinger, M., J. Kaltenbacher. (2015, 10). Aeroacoustics of Darrieus wind turbine. *International Journal of Aeroacoustics*, *14*, 883-902. doi: 10.1260/1475-472X.14.5-6.883